A mixed and multi-step higher-order implicit time integration family

M Rezaiee-Pajand* and **S R Sarafrazi**
Department of Civil Engineering, Ferdowsi University of Mashhad, Mashhad, Iran

The manuscript was received on 9 November 2009 and was accepted after revision for publication on 11 January 2010.

DOI: 10.1243/09544062JMES2093

Abstract: This article develops a new time integration family for second-order dynamic equations. A combination of the trapezoidal rule and higher-order Newton backward extrapolation functions are utilized in the formulation. Five members of the suggested family are extensively studied in this article. Most members of the presented time integration family are new. The stability and accuracy of the proposed time integration schemes are investigated by solving some benchmark problems. Numerical results are checked and compared with well-known strategies. The findings of the article show the efficiency, accuracy and robustness of the suggested techniques.

Keywords: time integration, multi-step, higher-order, implicit, non-linear analysis, dynamic relaxation, structural dynamics

1 INTRODUCTION

Numerical step-by-step time integration algorithms are widely used for structural dynamic analysis. These methods divide the time domain into many small steps. Afterwards, the variables at the end of each step are obtained using extrapolation functions for accelerations and velocities, which satisfy the equilibrium dynamic equations. The extrapolation functions may be written in terms of the previous known variables. Such methods are called explicit tactics. Performing a dynamic analysis by these schemes is very simple. However, the numerical instability is the most crucial difficulty in this group's application. In a time-consuming strategy, a very small time step should be utilized for analysing the non-linear problems [**1**]. To overcome this kind of difficulties, several researches have been developed so far [**2**–**5**].

On the other hand, there are the implicit procedures. The unknown variables at the end of the each time step inserted in the extrapolation functions belong to these methods. Consequently, the implicit processes result in more accurate solutions than the explicit ones. The most famous implicit algorithm is the Newmark method [**6**]. Because of the simplicity and the second-order accuracy, the Newmark technique is widely used for practical problems [**7**]. However, the restrictive stability conditions may reduce the abilities of this method for non-linear analysis. Therefore, many researchers have tried to improve the Newmark scheme. Some of them have introduced extra parameters to enforce the numerical damping and reduce the destructive effects of the high-frequency modes [**8**–**12**]. Some other researchers have utilized higher-order methods to achieve a good accuracy in the long time analysis. It should be noted, using the higher-order interpolation functions preserve the system energy and momentum too [**13**]. The coefficients of the higher-order polynomials can be obtained by utilizing the previous accelerations [**14**]. Using the Galerkin method and satisfying a weak form of the dynamic equilibrium equations, or using the points collocations scheme, are the other techniques to find the unknown coefficients [**15**–**20**]. In a newly published article, Soleymani *et al.* [**21**] employed the cubic spline reproducing kernel function to construct higher-order interpolation functions for linear analysis.

Bearing this in mind, the exact solution of the first-order differential equation is available. This is the solution of the single-degree system too, which can be easily introduced in terms of the exponential function. It is evident that extending this solution to a system with multiple degrees of freedom is not simple.

* *Corresponding author: Department of Civil Engineering, Ferdowsi University of Mashhad, P.O. Box 91775-1111, Mashhad, Iran.*
email: rezaiee@um.ac.ir; mrpajand@yahoo.com

In fact, it requires computing the exponential matrix. The Padé approximate function has been used for this purpose by researchers such as Möller [**22**] and Fung [**13, 23–26**]. Recently, Wang and Au [**27**] utilized the Padé approximation and the Gauss integration methods and proposed a very accurate time integration scheme.

To perform time integration, higher-order tactics are also developed, which require multi-step algorithms. The earliest work was carried out by Dahlquist [**28**], who employed the information of the previous steps to propose a multi-step process for analysis of the first-order differential equations. It is reminded, the simple way to calculate an integration is the trapezoidal rule, in which the variation of a function is assumed to be piecewise linear. Dahlquist utilized linear combinations of this rule for some sequential steps. Austin took advantage of the Newmark tactic for some subdomains [**29**]. He then used the Romberg sequence to improve the responses. However, this method is unstable and very small values for the time steps are required [**25**]. The multi-step algorithms usually have some additional parameters. The additional relations, which are rooted on analysts' experiences or mathematical bases, are required to find these parameters. In contrast to this, a multi-step tactic was presented by Bathe, which does not require supplementary conditions [**7**]. This algorithm has two sub-steps. The trapezoidal rule and the three-point Euler backward interpolations were utilized in its first and second stages, respectively.

Tarnow and Simo [**30**] employed two points, after and before the time step, respectively. They performed the Newmark technique for three stages of the lengths $\alpha\Delta t$, $(1-2\alpha)\Delta t$ and $\alpha\Delta t$, and obtained a fourth-order accuracy method. Another multi-step scheme was proposed by Fung [**25**]. For a free oscillation system, the Newmark process relates the displacements, velocities, and accelerations at the end of the time step to the known variables by using a coefficient matrix. Fung utilized a linear combination of the coefficient matrices, which are calculated for the sub-stages. By comparing the accuracy of the obtained interpolation with the Taylor series, he found the weighted parameters. Moreover, the extreme value of the spectral radius of the coefficient matrix was considered, too.

The idea of utilizing a multi-step algorithm and the mixed interpolation functions is the basis of the present investigation. In this study, a new family for the time integration is introduced. In the first sub-step of this family, the trapezoidal rule is utilized. The other stages of the suggested technique take advantage of the higher-order Newton interpolations for derivatives. The combination of the proposed family and the dynamic relaxation method (DRM) present a very simple and applicable procedure. The efficiency of the new method is verified by its application to a wide range of the mechanical systems and structural dynamic problems, with linear and non-linear behaviours. Due to volume limitation, only a few benchmark problems are presented in this article. The results show that the proposed formulation improves the accuracy and the robustness of the analysis considerably, as compared with the other well-known strategies.

2 THE TWO-STAGE ALGORITHM

The governing relationships of a structural dynamic system are a set of the second-order differential equations. A general tactic for solving this problem is the numerical time integration. This process utilizes a very small fraction of the total time domain, as the length of the integration step. Afterwards, the dynamic equilibrium equations are usually satisfied at the specific points of the time domain. A sample of the dynamic equations is written at the end of the nth time step in the equation below

$$\mathbf{M}\ddot{\boldsymbol{X}}^{n+1} + \mathbf{C}^{n+1}\dot{\boldsymbol{X}}^{n+1} + \mathbf{S}^{n+1}\boldsymbol{X}^{n+1} = \boldsymbol{P}^{n+1} \tag{1}$$

In this equation, **M**, **C**, and **S** are mass, damping, and the stiffness matrices, respectively, and $\boldsymbol{P}$ is the structural load vector. The displacements, velocities and accelerations are shown by $\boldsymbol{X}$, $\dot{\boldsymbol{X}}$, and $\ddot{\boldsymbol{X}}$, respectively. These variables are unknown at the end of the time step. In the implicit techniques, the velocities and accelerations are usually extrapolated by two functions in the terms of the previous known parameters and the unknown displacements $\boldsymbol{X}^{n+1}$. The second-order accuracy time integration methods use the displacements, velocities, and accelerations at time t_n as the known variables. On the other hand, the higher-order methods require more known conditions.

Recently, Bathe proposed a second-order process, which has two stages [**7**]. It is denoted by BM2 in the present article. Using the trapezoidal rule in the first stage, the unknown variables are evaluated at time $t_n + \Delta t/2$. In other words, the time step is divided into two equal segments and the trapezoidal rule is used in the first one. When the first stage is completed, the variables at time $t_{n+1/2}$ are known. Afterwards, by using the available data at two points, t_n and $t_{n+1/2}$, the Euler backward interpolation can be formed to extrapolate the nodal variables at time $t_n + \Delta t$. The mathematical formulas of the aforementioned procedure are presented in the following forms

$$\text{Stage 1}: \begin{cases} \dot{\boldsymbol{X}}^{n+1/2} = \dfrac{4}{\Delta t}\left(\boldsymbol{X}^{n+1/2} - \boldsymbol{X}^{n}\right) - \dot{\boldsymbol{X}}^{n} \\ \ddot{\boldsymbol{X}}^{n+1/2} = \dfrac{4}{\Delta t}\left(\dot{\boldsymbol{X}}^{n+1/2} - \dot{\boldsymbol{X}}^{n}\right) - \ddot{\boldsymbol{X}}^{n} \end{cases}$$

$$\text{Stage 2}: \begin{cases} \dot{\boldsymbol{X}}^{n+1} = \dfrac{3}{\Delta t}\boldsymbol{X}^{n+1} - \dfrac{4}{\Delta t}\boldsymbol{X}^{n+1/2} + \dfrac{1}{\Delta t}\boldsymbol{X}^{n} \\ \ddot{\boldsymbol{X}}^{n+1} = \dfrac{3}{\Delta t}\dot{\boldsymbol{X}}^{n+1} - \dfrac{4}{\Delta t}\dot{\boldsymbol{X}}^{n+1/2} + \dfrac{1}{\Delta t}\dot{\boldsymbol{X}}^{n} \end{cases} \tag{2}$$

Bathe stated that the BM2 technique can conserve the energy and momentum through the dynamic analysis [**7**]. The idea of utilizing a multi-step algorithm and the mixed interpolation functions are the bases of this investigation. A new time integration family is introduced in this study. The details of the formulation for the proposed family are presented in the next section.

3 THE PROPOSED FAMILY

It is worth emphasizing that the three-point Euler backward interpolation is a special case of the Newton backward divided difference formula. This property is employed to develop a new time integration family. To establish the formulation, the time step is divided into m equal segments, as shown in Fig. 1. One can assume that the nodal values of a function, such as Z, are known. Based on this, the m+1 sample points can be utilized to write the m-order Newton interpolation function as follows

$$Z(t) = [z_n] + [z_n, z_{n+1/m}](t - t_n) + \cdots + [z_n, z_{n+1/m}, \ldots, z_{n+1}](t - t_n)(t - t_{n+1/m}) \cdots (t - t_{n+1-1/m}) \tag{3}$$

where the coefficients $[z_n, z_{n+1/m}, \ldots, z_{n+i/m}]$ are functions of the sample values and the length of the segments. One can calculate the first derivative of Z and substitute $t_n + (i/m)\Delta t$ instead of t to find $\dot{Z}^{n+(i/m)}$ as below

$$\dot{Z}^{n+(i/m)} = \frac{m}{i!\Delta t}\sum_{j=0}^{i} N_{ij} Z^{n+(j/m)}, \quad i = 2, 3, \ldots, m \tag{4}$$

where N_{ij} are the coefficients of the Newton interpolation for the first derivative. The parameters of the

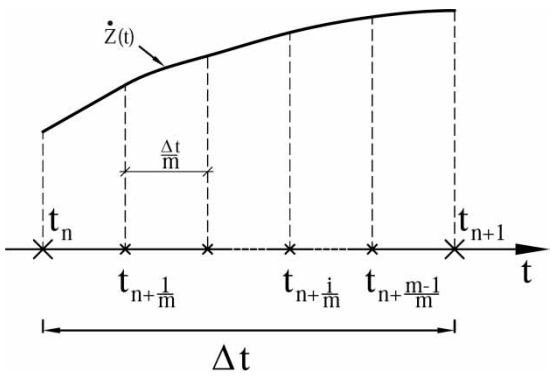

Fig. 1 The sub-domains of the time step

Table 1 The coefficients of the Newton interpolation for the first derivative

i	N_{i0}	N_{i1}	N_{i2}	N_{i3}	N_{i4}	N_{i5}	N_{i6}
1	−1	1	–	–	–	–	–
2	1	−4	3	–	–	–	–
3	−2	9	−18	11	–	–	–
4	6	−32	72	−96	50	–	–
5	−24	150	−400	600	−600	274	–
6	120	−864	2700	−4800	5400	−4320	1764

first- to sixth-order functions are obtained and inserted in Table 1.

Relation (4) is used to interpolate the velocity and acceleration. In other words, if the displacement vector is substituted in equation (4), instead of Z, the velocity vector at time $t = t_n + (i/m)\Delta t$ is obtained. The acceleration is similarly extrapolated in terms of the velocities, when the $\dot{\boldsymbol{X}}$ vector is substituted for scalar parameter Z. This study shows that using the first-order Newton interpolation for the first sub-stage causes a considerable numerical damping. On the other hand, utilizing the trapezoidal rule presents better solutions. Therefore, the extrapolation functions in the first stage are written in the following form

$$\begin{cases} \dot{\boldsymbol{X}}^{n+(1/m)} = \dfrac{2m}{\Delta t}\left(\boldsymbol{X}^{n+(1/m)} - \boldsymbol{X}^{n}\right) - \dot{\boldsymbol{X}}^{n} \\ \ddot{\boldsymbol{X}}^{n+(1/m)} = \dfrac{2m}{\Delta t}\left(\dot{\boldsymbol{X}}^{n+(1/m)} - \dot{\boldsymbol{X}}^{n}\right) - \ddot{\boldsymbol{X}}^{n} \end{cases} \tag{5}$$

The extrapolation functions in the other stages are written in the form of equation (4). The results are as below

$$\begin{cases} \dot{\boldsymbol{X}}^{n+(i/m)} = \alpha_{ii}\boldsymbol{X}^{n+(i/m)} + \displaystyle\sum_{j=0}^{i-1}\alpha_{ij}\boldsymbol{X}^{n+(j/m)} \\ \ddot{\boldsymbol{X}}^{n+(i/m)} = \alpha_{ii}^2\boldsymbol{X}^{n+(i/m)} + \displaystyle\sum_{j=0}^{i-1}\alpha_{ij}\left(\dot{\boldsymbol{X}}^{n+(j/m)} + \alpha_{ii}\boldsymbol{X}^{n+(j/m)}\right) \\ \alpha_{ij} = \dfrac{m}{i!\Delta t}N_{ij}, \quad i = 2, 3, \ldots, m, \quad j = 0, 1, \ldots, i \end{cases} \tag{6}$$

The system variables at time $t = t_n + i\,\Delta t/m, i = 1, 2, \ldots, m$, should satisfy the dynamic equilibrium equations. Consequently, the velocities and accelerations of equations (5) or (6) are substituted into equation (1), and the governing equation is written in terms of the unknown displacements as follows

$$\begin{aligned} &\mathbf{S}_{\text{eq}}\boldsymbol{X}^{n+(i/m)} = \boldsymbol{P}_{\text{eq}} \\ &\mathbf{S}_{\text{eq}} = \mathbf{S}^{n+(i/m)} + \alpha_{ii}^2\mathbf{M} + \alpha_{ii}\mathbf{C}^{n+(i/m)} \\ &\boldsymbol{P}_{\text{eq}} = \boldsymbol{P}^{n+(i/m)} - \mathbf{M}\boldsymbol{f}_1^{n+(i/m)} - \mathbf{C}^{n+(i/m)}\boldsymbol{f}_2^{n+(i/m)} \end{aligned} \tag{7}$$

where $\boldsymbol{f}_1$ and $\boldsymbol{f}_2$ are two functions of the previous variables, and they are written for the first stage as below

$$\begin{cases} \boldsymbol{f}_1^{n+(1/m)} = -\alpha_{10}^2 \boldsymbol{X}^n - 2\alpha_{10}\dot{\boldsymbol{X}}^n - \ddot{\boldsymbol{X}}^n \\ \boldsymbol{f}_2^{n+(1/m)} = -\alpha_{10}\boldsymbol{X}^n - \dot{\boldsymbol{X}}^n \\ \alpha_{10} = \dfrac{2m}{\Delta t} \end{cases} \tag{8}$$

The parameters $\boldsymbol{f}_1$ and $\boldsymbol{f}_2$ in the other stages are obtained by utilizing the following relations

$$\begin{cases} \boldsymbol{f}_1^{n+(i/m)} = \displaystyle\sum_{j=0}^{i-1} \alpha_{ij} \left(\dot{\boldsymbol{X}}^{n+(j/m)} + \alpha_{ii} \boldsymbol{X}^{n+(j/m)} \right) \\ \boldsymbol{f}_2^{n+(i/m)} = \displaystyle\sum_{j=0}^{i-1} \alpha_{ij} \boldsymbol{X}^{n+(j/m)} \\ i = 2, 3, \ldots, m \end{cases} \tag{9}$$

Equivalent static system of equation (7) requires the load vector at the ith point of the sub-region. This vector can be linearly interpolated between the values of the load vector at two ends of the time step as below

$$\boldsymbol{P}^{n+(i/m)} = \left(1 - \frac{i}{m}\right) \boldsymbol{P}^n + \frac{i}{m} \boldsymbol{P}^{n+1} \tag{10}$$

It is clear that using equation (10) can insert some errors in the responses. If the values of the load vector at the middle points are available, employing the exact values improves the results. Up to here, all the required relations for solving the dynamic system are available. These equations are forming a new algorithm. In other words, the aforementioned relations are programmed and a family of the numerical time integrations is obtained. When the value of the parameter m is 2, the BM2 process is resulted. All the family members with more than two sub-stages are new. The stability and accuracy of three-, four-, five- and six-stage methods of the proposed multi-step time integration family are studied in the next sections.

4 VERIFYING THE STABILITY

The stability of the suggested time integration family is studied in this section. This goal can usually be reached by verifying an un-damped and free oscillation of a single-degree-of-freedom (SDOF) system. The results of studying an SDOF structure could be extended for most of the structures [**31**]. According to the literatures, this is not a sufficient condition for a general non-linear dynamic problem. A dynamic equilibrium equation of an un-damped SDOF is considered as below

$$\ddot{x} + \omega^2 x = 0 \tag{11}$$

where ω is the natural angular frequency of vibration. From an analytical point of view, the numerical time integration scheme is an iterative process, which calculates the displacement, velocity, and acceleration at time $t_n + \Delta t$ in terms of previous data. One available method to study the stability of such procedure is verifying the spectral radius of the system coefficient matrix. The mentioned matrix relates the unknown variables to the previous known ones in the following form

$$\begin{Bmatrix} x \\ \dot{x} \\ \ddot{x} \end{Bmatrix}^{n+1} = \mathbf{A} \begin{Bmatrix} x \\ \dot{x} \\ \ddot{x} \end{Bmatrix}^{n} \approx \boldsymbol{Y}^{n+1} = \mathbf{A}\boldsymbol{Y}^n \tag{12}$$

Combining the extrapolations of equations (5) and (6) with the equilibrium equation (11), matrix $\mathbf{A}$ is obtained. The necessary condition for the stability of the iterative relation (12) is written as below

$$\rho(\mathbf{A}) = \max |\lambda_i| \leqslant 1 \tag{13}$$

The parameter ρ is called the spectral radius of $\mathbf{A}$. It is obvious, the solution becomes $\boldsymbol{Y}^{n+r} = \mathbf{A}^r \boldsymbol{Y}^n$, after performing the r steps. Recall that the eigenvalues of $\mathbf{A}^r$ are λ_i^r. Consequently, $\mathbf{A}^n$ is bounded when λ_i and λ_i^n are bounded too. In other words, restricting the spectral radius prevents the solution from unsteady growth. The value $\rho = 1$ for the un-damped SDOF system means that the amplitude is not changed as the time is elapsed. On the other hand, the solution approaches to zero when the spectral radius is less than one. It should be noted, matrix $\mathbf{A}$ depends on the values of the system's natural period, $T = 2\pi/\omega$, and time step. It is customary to present the spectral radius in terms of $\Delta t/T$ ratio. In this article, the spectral radius for the proposed family is calculated numerically. Figure 2 shows the curves of ρ versus the $\Delta t/T$ ratio, for different values of m. The curve of the spectral radius for the linear acceleration method of Newmark is also presented in Fig. 2.

As it is shown in Fig. 2, the spectral radius of Newmark process, between $\Delta t = 0$ and $0.5513T$, remains

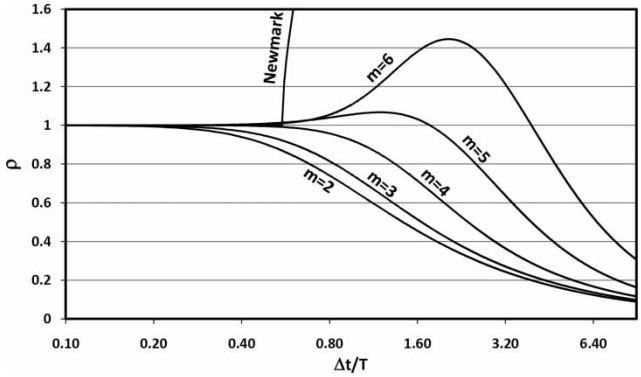

Fig. 2 The curves of spectral radius

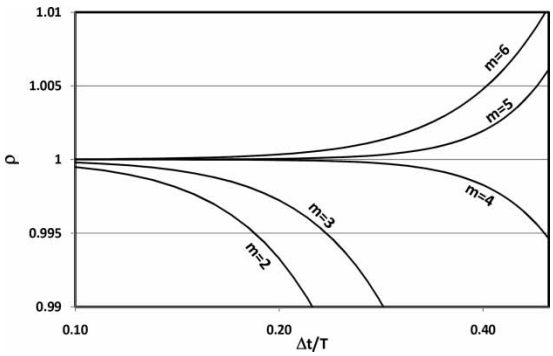

Fig. 3 The curves of spectral radius

1. Out of this region, it suddenly increases. The mentioned behaviour has been also reported by some other authors [**32**]. It is worth emphasizing that the variation of the spectral radius between 0 and $0.5\Delta t/T$ is very important. This part of the curves is shown in Fig. 3 in more detail.

Figure 3 shows that the five- and six-step members of the presented family are not always stable. Even for a small value of the $\Delta t/T$ ratio, the value of the spectral radius for these algorithms is greater than one. However, for the applicable domains, ρ is a little more than one. It should be noted, in most cases of the multi-degree-of-freedom systems, there are numerical dampings and some instability domains are usually eliminated. Altogether, from the stability point of view, the five- and six-order schemes behave near the linear acceleration strategy of Newmark. On the other hand, the family members with the orders 3 and 4 are stable. In fact, for a large value of $\Delta t/T$, the value of the spectral radius of these members is very close to one. The numerical outcomes also indicate the good capability and the accuracy of these schemes.

The spectral radius is also used to study the dissipation in the numerical time integration algorithm. A suitable tactic should conserve the energy of the low-frequency responses. Consequently, the curve of the spectral radius should be very near to the line $\rho = 1$, for the small $\Delta t/T$ ratios. From this point of view, the three- and four-step members of the proposed family behave much better than the BM2 approach. On the other hand, the high frequencies may cause instability. Therefore, the high-frequency modes should be damped. It means that the spectral radius would be less than one for the large values of the $\Delta t/T$ ratio. Researchers have suggested that the extreme value of the spectral radius should be kept in the domain of 0.5–0.8 when the value of the time step is tending to infinity [**25**]. The new multi-step time integration techniques, and also BM2 tactic, have the same behaviour for very high modes. In fact, the curves of the spectral radii are approaching zero for all the aforementioned procedures.

5 DYNAMIC ANALYSIS USING THE DYNAMIC RELAXATION METHOD

Dynamic analysis requires solving a static system of equations in each step. The Newton–Raphson or Gauss–Seidel iteration methods can solve these equations [**15**, **33**]. Rezaiee-Pajand and Alamatian utilized the dynamic relaxation technique to solve non-linear dynamic problems [**34**]. It is reminded that the DRM is an algorithm for solving a system of linear or non-linear static equations. The DRM solver adds the inertia and damping forces to the static system. Starting from initial values for the unknowns, the central finite difference method is used to find the steady state of the pseudo-dynamic system. In this section, a modified DR algorithm for solving the dynamic problems is utilized, which is slightly different from reference [**34**]. At first, two orthogonal time axes are assumed. The dynamic relaxation time axis is denoted by τ, and the axis t shows the real time. The fictitious mass and damping matrices are $\mathbf{M}_{\mathrm{F}}$ and $\mathbf{C}_{\mathrm{F}}$, respectively. It is evident that the system has the real damping and masses too. Therefore, the responses of the structure are functions of both real and artificial times. The equilibrium equation of such a system at the time (t_{n+1}, τ_k) is written in the following form

$$\mathbf{M}_{\mathrm{F}}^{n+1,k}\boldsymbol{X}_{,\tau\,\tau}^{n+1,k} + \mathbf{C}_{\mathrm{F}}^{n+1,k}\boldsymbol{X}_{,\tau}^{n+1,k} + \mathbf{M}\boldsymbol{X}_{,t\,t}^{n+1,k} + \mathbf{C}^{n+1,k}\boldsymbol{X}_{,t}^{n+1,k} + \mathbf{S}^{n+1,k}\boldsymbol{X}^{n+1,k} = \boldsymbol{P}^{n+1,k} \tag{14}$$

For simplicity, the velocity and acceleration are shown by the subscripted displacement vector. Using a numerical time integration strategy, the system of differential equation (14) is solved in the real-time space. At time t_{n+1}, the system is released from $\boldsymbol{X}^n$ location. For the time on which the dynamic equilibrium equations are not satisfied, the system is vibrated in the spurious time space. When the system reaches the steady state, the correct solution of $\boldsymbol{X}^{n+1}$ is found. It should be reminded that the DRM uses the central finite difference process to obtain the equilibrium state. The mentioned algorithm is performed in the following stages.

1. Define $\alpha_{m\,j}, j = 0, 1, \ldots, i$.
2. Take $k = 0$ and $\boldsymbol{X}^{n+1,k} = \boldsymbol{X}^n$.
3. Calculate the real velocities $\boldsymbol{X}_{,t}^{n+1,k}$ and accelerations $\boldsymbol{X}_{,t\,t}^{n+1,k}$ using equations (5) or (6).
4. Update the real stiffness $\mathbf{S}^{n+1,k}$, damping $\mathbf{C}^{n+1,k}$ and loads $\boldsymbol{P}^{n+1,k}$.
5. Calculate the residual dynamic forces from the formula below

$$\boldsymbol{R}^{n+1,k} = \boldsymbol{P}^{n+1,k} - \mathbf{M}\boldsymbol{X}_{,t\,t}^{n+1,k} - \mathbf{C}^{n+1,k}\boldsymbol{X}_{,t}^{n+1,k} - \mathbf{S}^{n+1,k}\boldsymbol{X}^{n+1,k}$$

6. Compute the fictitious mass matrix $\mathbf{M}_{\mathrm{F}}^{n+1,k}$ and damping factor c_{f}^{k}.
7. Calculate spurious velocities

$$\boldsymbol{X}_{,\tau}^{n+1,k+1/2} = \frac{2 - c_{\mathrm{f}}^{k}\Delta\tau_k}{2 + c_{\mathrm{f}}^{k}\Delta\tau_k}\boldsymbol{X}_{,\tau}^{n+1,k-1/2} + \frac{2}{2 + c_{\mathrm{f}}^{k}\Delta\tau_k}\mathbf{M}_{\mathrm{F}}^{-1}\boldsymbol{R}^{n+1,k}$$

8. Obtain a new displacement using $\boldsymbol{X}^{n+1,k+1} = \boldsymbol{X}^{n+1,k} + \Delta\tau_k \boldsymbol{X}_{,\tau}^{n+1,k+1/2}$.
9. Check the value of $\|\boldsymbol{R}^{n+1,k+1}\|$. If it is greater than the acceptable error ε_R, repeat the iteration from statement (3). Otherwise, the DR process has converged and a new sub-stage or the next step is started.

The values of the fictitious matrices, damping and masses, should be chosen such that the artificial dynamic system converges to the solution $\boldsymbol{X}^{n+1}$, as soon as possible. Consequently, the critical damping should be applied. In the aforementioned algorithm, parameter c_{f} is the critical damping factor. It should be noted, the damping matrix of DRM is written in terms of the fictitious mass matrix, $\mathbf{C}_{\mathrm{F}} = c_{\mathrm{f}}\ \mathbf{M}_{\mathrm{F}}$ [**35**]. The Rayleigh tactic is a common method for finding the critical damping factor, which can be written as below [**34**]

$$c_{\mathrm{f}} = 2\sqrt{\frac{\boldsymbol{X}^{\mathrm{T}}\{\alpha_{ii}^2\mathbf{M}\boldsymbol{X} + \alpha_{ii}\mathbf{C}\boldsymbol{X} + \mathbf{S}\boldsymbol{X}\}}{\boldsymbol{X}^{\mathrm{T}}\mathbf{M}_{\mathrm{F}}\boldsymbol{X}}} \leqslant 2/\Delta\tau_k \tag{15}$$

To easily invert the matrix $\mathbf{M}_{\mathrm{F}}$, a diagonal matrix is chosen as follows [**36**]

$$mf_{ii} = \frac{\psi}{4}\sum_j \left(|s_{ij}| + \alpha_{ii}^2|m_{ij}| + \alpha_{ii}|c_{ij}|\right) \tag{16}$$

where ψ is a parameter greater than 1, and usually is assumed to be equal to 1.1, according to Papadrakakis's suggestion [**37**]. For simplifying the algorithm, the non-diagonal terms of the real matrices are ignored, and 2 is used for the parameter ψ. It is worth emphasizing, there is no requirement to multiply $\mathbf{S}$ in $\boldsymbol{X}$. Because the resulting vector is the vector of the internal forces, it is calculated at the elements assembling level. In addition, there are no column or row operations over the matrices in the DRM relations. Consequently, the non-zero elements of the upper triangular matrices are stored in the vectors to reduce the total number of operations and required memories.

6 NUMERICAL EXAMPLES

The stability and accuracy of the proposed time integration schemes are discussed by solving some problems. The results are checked and compared with the well-known strategies. The constant and linear acceleration algorithms of Newmark [**6**] and the Wilson-θ process [**8**] are three well-known procedures. These time integration procedures are named by Newmark constant acceleration method (NCA), Newmark linear acceleration method (NLA), and Wilson theta method (WTM), respectively. The extensive numerical studies show that accurate results are obtained using three- and four-step members of the proposed family.

6.1 The van der Pol equation

The van der Pol equation is solved as the first example. This study exposes the phase difference error for the suggested schemes. The results are compared with NLA, WTM, and BM2 tactics. The van der Pol equation is written as below

$$\ddot{x} - \mu(1 - x^2)\dot{x} + x = 0, \quad x^0 = 2, \quad \dot{x}^0 = 0, \quad \mu = 0.1$$

The exact solution for this system has the following form

$$x = \left(x^0 - \frac{\mu^2}{8}\right)\cos(\omega t) + \frac{3}{4}\mu\sin(\omega t) + \frac{3}{16} \times \mu^2\cos(3\omega t) - \frac{1}{4}\mu\sin(3\omega t) - \frac{1}{16}\mu^2\cos(5\omega t)$$

$$\omega = 1 - \frac{\mu^2}{16}$$

The three- to six-step tactics of the new family are used as a tool for the time integration. It should be reminded that the two-step family member is the same as the BM2 scheme. In this investigation, the differences between the exact displacements and those found by numerical integration describe the errors. The errors are also normalized with respect to the maximum value of displacement. It is clear that the values of the errors are also fluctuated. Whereas the total time, $t = 600$ s, is much larger than the period of the system, the curves of the errors present a cramped figure. For this problem, the envelope curves of the positive normalized errors are plotted in Fig. 4. In this case, all the

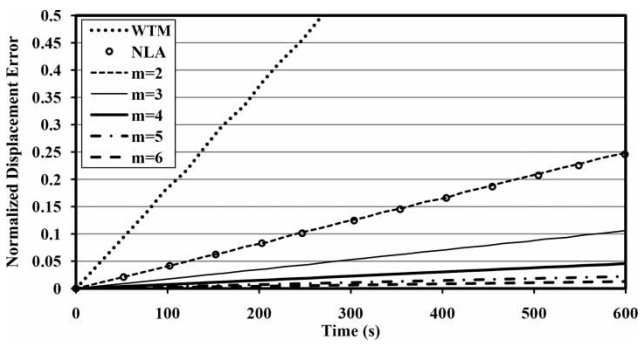

Fig. 4 The envelope curves of the normalized displacement errors

time integration processes use the time step equal to $\Delta t = 0.1$ s.

According to Fig. 4, the Wilson-θ approach gives the worst results. The Newmark [**6**] and Bathe [**7**] algorithms present the same error in this example. Furthermore, the errors reduce when the order of integration increases. In this example, the NLA errors are approximately five times of the four-step strategy errors. However, the analysis time used by the four-step approach is almost four times the NLA one. This indicates the efficiency of the presented formulation. As it was mentioned previously, the time steps are the same for all procedures. Consequently, the higher-order techniques use the smaller sub-step. It is suitable to study the effect of sub-step size on the accuracy of the results. To find this effect, the problem is solved by different values of the time step, so that the continuances of the sub-stages are equal in all aforementioned algorithms. In other words, the time step for the m-step scheme is chosen as 0.1 m. Figure 5 shows the displacements curves between 595 and 600 s.

As shown in Fig. 5, the best result is obtained by using the Newmark linear acceleration scheme. The findings demonstrate that the analyst cannot achieve a better accuracy by increasing the sub-steps when the value of the time step increases with the same rate. However, the Newmark method is only stable for the specific time step values, but some of the higher-order algorithms are unconditionally stable. Figure 5 also shows the displacement errors in all schemes, which result from the period errors. It is seen that the Newmark method gives the best result for equal sub-steps; the WTM presents the worst solutions in both equal and unequal sub-regions. In other tactics, the outcome accuracy is increased when the number of sub-steps increases.

6.2 2D non-linear oscillator

The dynamic system of Fig. 6 is a combination of a concentrated mass, $m = 4$ kg, and a spring. The concentrated mass can rotate around the axis x_3 on the horizontal table without any friction. The stiffness and the initial length of the spring are $k = 10$ N/m and $L = 10$ m, respectively.

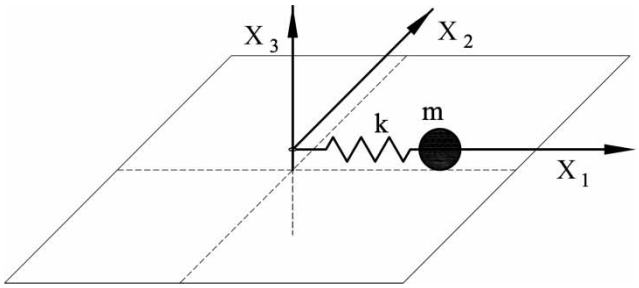

Fig. 6 The 2D non-linear oscillator

The dynamic equilibrium equations of this system can be written as below

$$\begin{bmatrix} m & 0 \\ 0 & m \end{bmatrix} \ddot{\boldsymbol{X}} + \begin{bmatrix} ka & 0 \\ 0 & ka \end{bmatrix} \boldsymbol{X} = \begin{Bmatrix} 0 \\ 0 \end{Bmatrix}$$

$$a = \frac{\sqrt{x_1^2 + x_2^2} - L}{\sqrt{x_1^2 + x_2^2}}$$

The motion of the mass is started by applying the initial velocity $\dot{x}_2^0 = 10$ m/s. Figure 7 shows the locus of the mass between 0 and 64 s, which is found by using the Newmark-β method and the time step equal to 0.1 s.

It is noted that the period of the system is approximately 6.4 s. Consequently, some non-linear dynamic analyses are performed using 0.6 s as the time step. A selected part of the solutions for the proposed time integration family and also for the BM2 and NLA schemes are presented in Fig. 8. The near-exact displacements are obtained by utilizing the NLA process and $\Delta t = 0.001$ s. The figure shows the good accuracy solutions for the fourth and the higher-order algorithms.

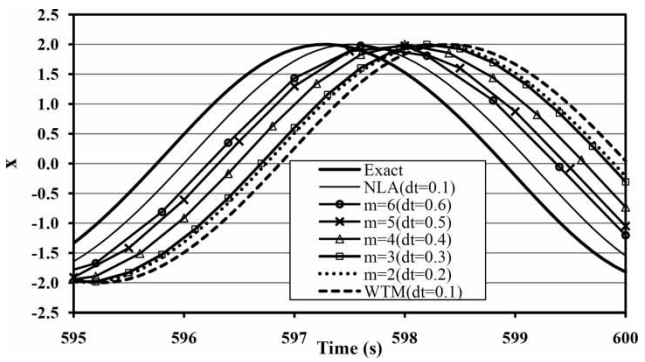

Fig. 5 The displacement curves

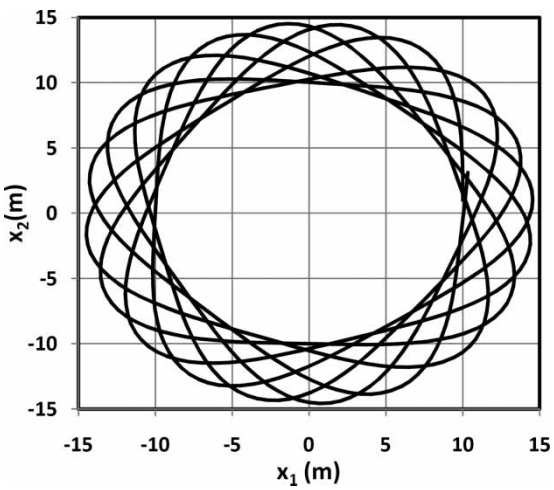

Fig. 7 The locus of the ball between 0 and 64 s

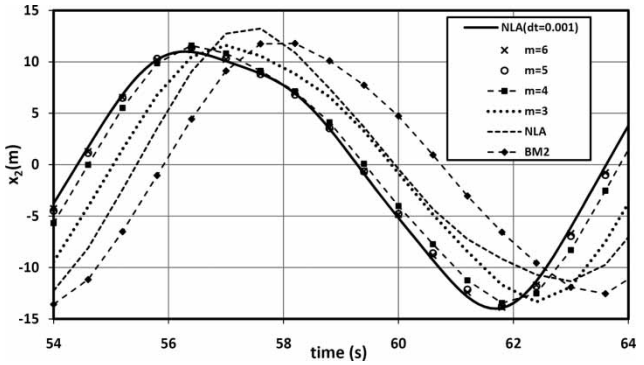

Fig. 8 The curves of the x_2 component of the displacements

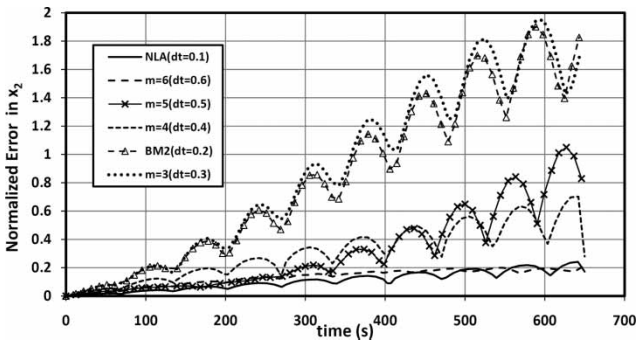

Fig. 9 The envelope curves of errors in x_2

In order to investigate the effect of smaller sub-steps on the accuracy of the higher-order schemes, some other analyses are performed by utilizing $\Delta t = 0.1$ m, between 0 and 650 s. The results are compared to the solutions of BM2 and NLA techniques, when using $\Delta t = 0.01$ and 0.002 s, respectively. Using a very smaller time step for NLA changes the solutions about a maximum of per cent 0.1. In other words, this solution is near exact. It is interesting to find the errors of the displacements. Figure 9 shows the envelope curves of the normalized errors in x_2 with respect to the maximum displacement. The result of this study is the same as the outcome of the previous section. In other words, among the mentioned schemes, the Newmark procedure is the best when the algorithms are stable and the lengths of the sub-steps for all techniques are equal. Outcomes of the six-step process are near the NLA ones. The five-step tactic is also better than the four-step method, since time is lesser than 400 s. After that, the four-step strategy answer has fewer errors. It is evident that the mentioned behaviour of the five-step procedure is due to weak numerical instability. In this example, the results of BM2 and the three-step methods have no quantitative difference.

6.3 The shear building

Figure 10 shows a five-story shear building, which is adopted from Wang [**27**]. The masses of all stories

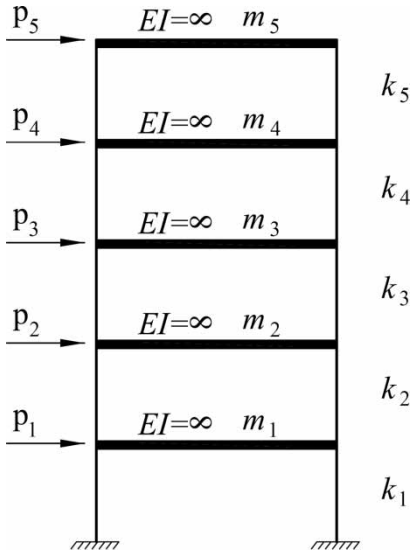

Fig. 10 The shear building

are the same, and equal to 2.616×10^6 kg. The stiffness of stories, k_2–k_5, is 981×10^6 N/m. The value of k_1 is 20 per cent more than the others. The damping matrix of the structure consists of the classical and additional parts. The classical damping matrix is obtained using $\mathbf{C}_c = 0.3\mathbf{M} + 0.002\mathbf{S}$. The additional term is $20\mathbf{C}_c(1,1)$, which is added to the first degree of freedom to consider a damper device at the first story. Five lateral forces affect the structure as shown in Fig. 10. The equation of these loads is given below

$$\boldsymbol{P} = 2.616 \times 10^6 \{1 \quad 1 \quad 1 \quad 1 \quad 1\}^{\mathrm{T}} \sin(\pi\, t)$$

This shear-type building is analysed by utilizing several time integration methods, with $\Delta t = 0.01$ s. The displacements and velocities at the top story of structure are arranged in Table 2. The very accurate results of the Gauss precise integration method (GPIM) process of Wang and Au [**27**] are also inserted in this table. Table 2 shows that the proposed family can present high accuracy solutions, whereas the simplicity of the suggested algorithms is preserved. Furthermore, one can increase the order of the method to improve the results. It should be reminded, the GPIM tactic uses the Padé approximation of the order (2, 2) for exponential matrix in the exact solution. The (2, 2)-order of this approximation is a rational function of two second-order polynomials. Its denominator is written in terms of the coefficient matrix for the equivalent first-order differential equations. Therefore, using this approximation requires calculating the inverse of a matrix. In order to avoid inverting process, Wang and Au utilized a ten-stage recurrence algorithm. All the aforementioned calculations should be performed at the five Gauss points for each step to obtain the solutions, which requires considerable time.

Table 2 The results of the shear building analysis at the roof

Scheme	Res.	Time 0.2	0.4	0.6	0.8	1	Max error (%)
Exact	x_5	0.004 036	0.026 384	0.053 295	0.054 803	0.019 810	
	$\dot{x}_5$	0.059 093	0.149 040	0.093 347	−0.089 965	−0.238 530	
GPIM	x_5	0.004 036	0.026 384	0.053 295	0.054 803	0.019 810	0.000
	$\dot{x}_5$	0.059 092	0.149 040	0.093 347	−0.089 965	−0.238 530	0.000
$m=6$	x_5	0.004 035	0.026 382	0.053 290	0.054 798	0.019 809	0.009
	$\dot{x}_5$	0.059 087	0.149 028	0.093 341	−0.089 953	−0.238 510	0.013
$m=5$	x_5	0.004 036	0.026 381	0.053 290	0.054 799	0.019 809	0.010
	$\dot{x}_5$	0.059 086	0.149 029	0.093 342	−0.089 949	−0.238 510	0.017
$m=4$	x_5	0.004 036	0.026 381	0.053 289	0.054 799	0.019 811	0.012
	$\dot{x}_5$	0.059 084	0.149 031	0.093 345	−0.089 941	−0.238 510	0.026
$m=3$	x_5	0.004 036	0.026 380	0.053 288	0.054 800	0.019 814	0.021
	$\dot{x}_5$	0.059 080	0.149 035	0.093 353	−0.089 921	−0.238 510	0.048
BM2	x_5	0.004 037	0.026 377	0.053 285	0.054 803	0.019 822	0.061
	$\dot{x}_5$	0.059 069	0.149 046	0.093 370	−0.089 872	−0.238 509	0.103
NCA	x_5	0.004 039	0.026 372	0.053 279	0.054 808	0.019 836	0.131
	$\dot{x}_5$	0.059 051	0.149 064	0.093 402	−0.089 786	−0.238 509	0.198
WTM	x_5	0.004 033	0.026 356	0.053 278	0.054 839	0.019 878	0.345
	$\dot{x}_5$	0.059 008	0.149 108	0.093 482	−0.089 566	−0.238 533	0.443

6.4 The 2-DOF system

Soleymani *et al.* [**21**] solved a problem with two degrees of freedoms, which is described as below

$$\begin{bmatrix} m & 0 \\ 0 & 3m \end{bmatrix} \ddot{\boldsymbol{X}} + \begin{bmatrix} 3k & -2k \\ -2k & 6k \end{bmatrix} \boldsymbol{X} = \begin{Bmatrix} 0 \\ f(t) \end{Bmatrix}$$

$$f(t) = \begin{cases} 1000\,(1 - 10\,t) & 0 \leqslant t \leqslant 0.1 \\ 0 & t > 0.1 \end{cases}$$

where the values of the stiffness coefficient k, and mass m are 1000 N/m and 0.5 kg, respectively. Utilizing the modal decomposition technique, Soleymani *et al.* found the exact solution. The natural frequencies and the mode matrix for the mentioned system are written in the following form

$$\begin{cases} \omega_1 = 49.834\,\text{rad/s} \\ \omega_2 = 87.700\,\text{rad/s} \end{cases}$$

$$\boldsymbol{\Phi} = \begin{bmatrix} 0.7783 & 1.1820 \\ 0.6825 & -0.4482 \end{bmatrix}$$

Assuming $\Delta t = 0.02$ s, the aforementioned system is solved by using several time integration methods. The solutions curves, between 0.8 and 1 s, are shown in Fig. 11. This figure shows that using the schemes with orders 4, 5, and 6, instead of NLA and BM2 processes, can much improve the solution. The Wilson-θ algorithm with $\theta = 1.42$ presents inaccurate results in this example. It is noted that Soleymani *et al.* obtained an accurate response by utilizing $\Delta t = 0.05$ s. However, they used the fourth-order accuracy functions and 11 collocations points. In other words, these researchers solved a system of 44 asymmetric equations in each step. Utilizing a new family of the time integration, only four symmetric systems, having two equations, are solved in the four-step proposed scheme.

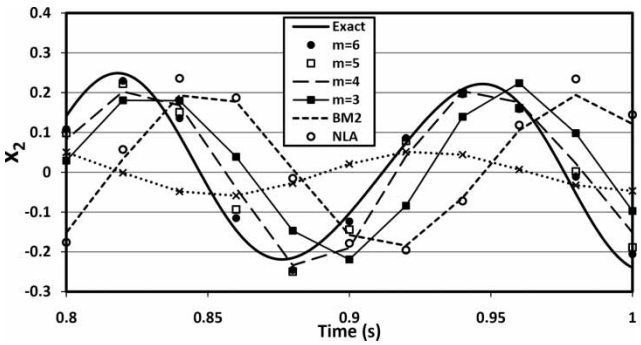

Fig. 11 The curves for the variation of x_2

6.5 The skew plate

In this section, a rhomboid plate bending with an acute angle of 30°, as shown in Fig. 12, is considered. The deflections of all peripheral nodes are fixed. Because of singularity in the bending moment at the acute angle, this structure is a very hard example and some finite element formulations cannot present the true solution. Accordingly, a suitable element, which

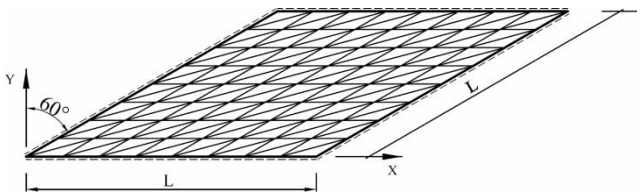

Fig. 12 The skew plate

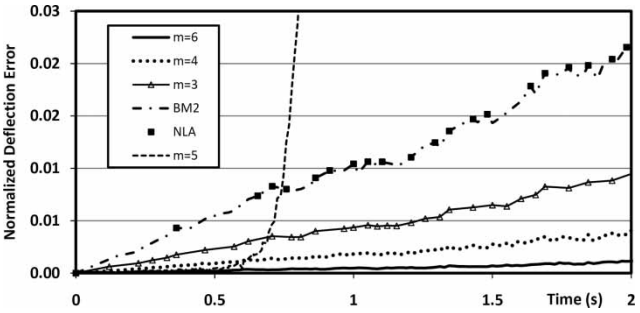

Fig. 13 The curves of the central displacements

was proposed by Onate *et al.* [**38**], is used to model the structure. The length, thickness and Poisson ratio for this structure are 10 m, 2 m, and 0.3, respectively. The modulus of elasticity and the value of the mass per volume of the plate are correspondingly chosen as 2×10^4 MPa and 10 KN s^2/m.

This plate is loaded by a uniformly distributed force, $q = q_0 \sin(2\pi t/0.019)$. The linear dynamic behaviour of the structure is studied between 0 and 2 s. The NLA scheme with a very small time step, $\Delta t = 5 \times 10^{-6}$ s, is utilized to find the near-exact solution. The proposed time integration processes are performed by using a time step of 0.0001 s. Figure 13 shows the envelope curves of the normalized error with respect to the extreme deflection.

Figure 13 shows that the values of the errors in the BM2 and NLA solutions are similar in this example. The sixth-order of the proposed family presents the best solution. However, performing more accurate studies show that this scheme is unstable, when the value of the time step is 0.000 15 s. The curve belonging to the fifth-order suggested technique in Fig. 13 indicates instability. It should be noted, the NLA method is also unstable when the value of the time step is 0.0002 s. The third- and the fourth-order algorithms are stable and produce accurate solutions. In the second part of this example, some other analyses are performed using larger time step, $\Delta t = 0.002$ s. The normalized result with respect to the extreme deflection is shown in Fig. 14. This figure includes the outcome of using the NLA process, with $\Delta t =$ 0.000 01 s, which is very close to the exact solution. According to Fig. 14, the BM2 procedure has a considerable period and amplitude errors. On the other hand, increasing the order of the new scheme to 4 can decrease the mentioned errors significantly.

The smallness of the sub-step length and order of the technique have affected the responses. These effects have been studied in the previous sections and are evaluated for the skew plate as well. Therefore, some analyses are carried out using different values for the time step as shown in Fig. 15. The length of the subregion is the same for all procedures. The solutions are compared with the results of NLA, with a time step of 3×10^{-6} s. It should be noted that the stiffness is very high and the linear behaviour is considered for the skew plate. Accordingly, very small time steps should be utilized to guarantee the stability of the five- and six-step methods and also NLA. Under these constraints, the values of errors are very small. As shown in Fig. 15, the errors are normalized with respect to the maximum error of the BM2 process to obtain comparable curves. The results verify the validity of

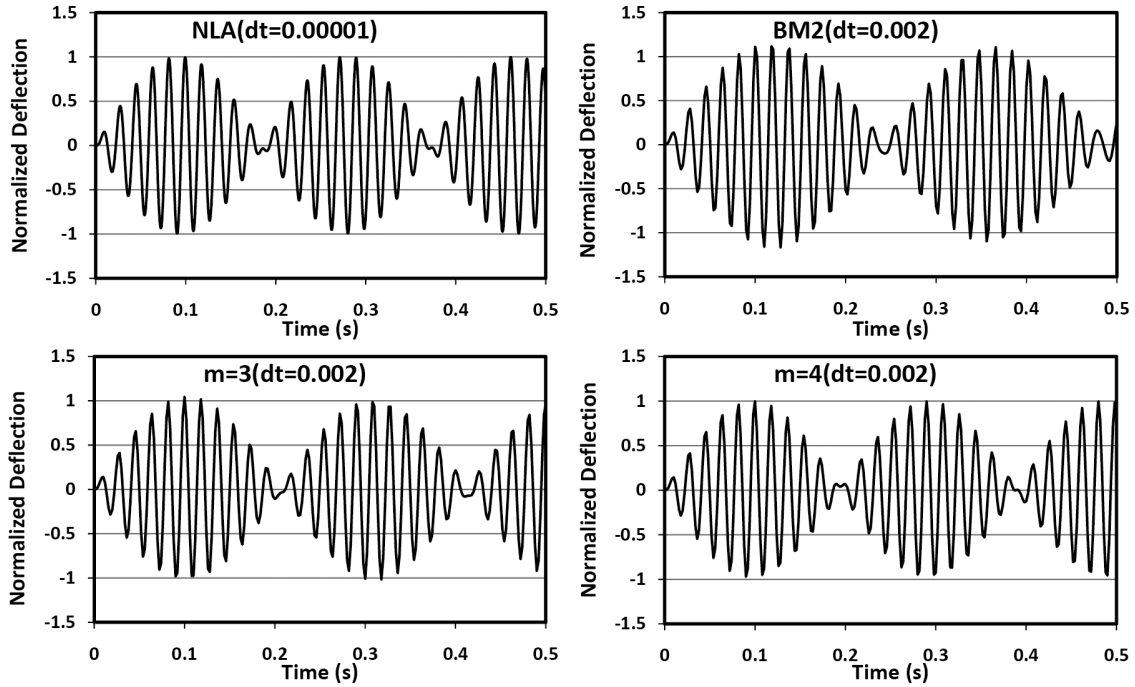

Fig. 14 The curves of the central displacements

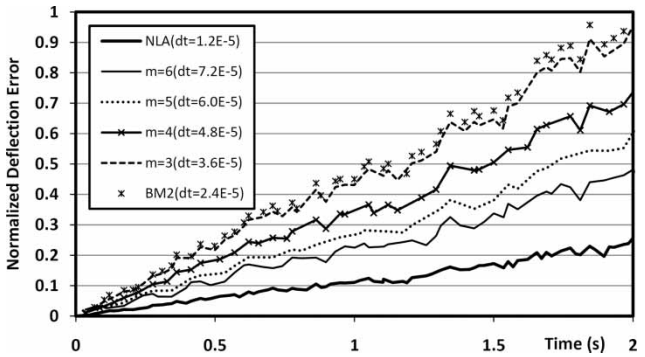

Fig. 15 The curves of the central displacements using different time step

the previous studies. In other words, the NLA scheme presents the best solutions. This study also shows that the accuracy usually decreases when the multiple processes with different orders are mixed in some of the sequential steps. However, utilizing the mixed orders may fulfill the stability requirements. The proposed mixed algorithms are effective when the time step is equal in all methods. It is worth mentioning that the analysis duration is seldom reported for the new methods. Usually, obtaining more accurate results requires more computational efforts. It should be reminded that one system of equations should be solved in each sub-step of the proposed family. Because considerable amount of calculation is devoted for solving equations, the higher-order tactics need more time. Furthermore, when the sub-step lengths are equal in all procedures, the required times are approximately the same.

7 CONCLUSIONS

A new family of a multi-step time integration scheme is presented. At first, the time step is divided into m equal segments. Afterwards, the system solutions at the end of the first segment are evaluated using the trapezoidal rule. The ith-order Newton interpolation for function derivative is used to calculate the structural responses at the ith internal point. It should be noted that a member of this family, which utilizes two sub-steps, is the same as the Bathe technique [**7**]. The three- to six-step members of the new algorithms are formulated and studied in this article. The stability of this family is verified using the spectral radius. The two, three, and four-step schemes are stable. However, those having five and six sub-steps are not always stable. In fact, the spectral radii of these conditionally stable procedures are very close to one, and they have a good performance when the time step is small enough. From the stability point of view, the five- and six-step methods behave similar to the Newmark scheme. The most important point is that the period errors for the proposed family decrease by using the strategies with more sub-steps. The numerical studies show that the responses of the two-stage Bathe method have usually the same accuracy as that of the Newmark one. On the other hand, the processes that utilize more sub-steps present the more accurate results.

In a very special case, when the lengths of the sub-steps for all aforementioned algorithms are the same, and the stability conditions for all procedures are fulfilled, the outcomes of the Newmark strategy usually have the best accuracy. It is to be regretted that this old tool has the stability deficiency! In comparison to the others, the two-step tactic has the most values of errors. However, the errors of all members of the newly suggested family decrease when the numbers of the sub-steps increase. It should be noticed, the required time for performing the integration procedures depends on the number of equations, which are solved in each sub-step. Consequently, when the lengths of sub-steps are the same for all tactics, the analysis durations are approximately the same. For instance, the analysis time used by the four-step approach is almost four times the NLA approach when the time step is the same for both the schemes. However, the NLA errors in Example 6.1 are five times of the four-step strategy errors. This indicates the efficiency of the presented formulation. Lastly, the Wilson-θ approach gives the worst results in both equal and unequal length of sub-steps.

REFERENCES

1 **Chang, S. Y.** and **Liao, W. I.** An unconditionally stable explicit method for structural dynamics. *J. Earthquake Eng.*, 2005, **9**(3), 349–370.

2 **Chang, S. Y.** Unconditional stability for explicit pseudodynamic testing. *Struct. Eng. Mech.*, 2004, **18**(4), 411–428.

3 **Rio, G., Soive, A.,** and **Grolleau, V.** Comparative study of numerical explicit time integration algorithms. *Adv. Eng. Softw.*, 2005, **36**, 252–265.

4 **Chang, S. Y.** Improved explicit method for structural dynamics. *J. Eng. Mech. ASCE*, 2007, **133**(7), 748–760.

5 **Rezaiee-Pajand, M.** and **Alamatian, J.** Numerical time integration for dynamic analysis using a new higher order predictor-corrector method. *Eng. Comp.*, 2008, **25**(6), 541–568.

6 **Newmark, N. M.** A method of computation for structural dynamics. *J. Eng. Mech. Div. ASCE*, 1959, **85**(EM3), 67–94.

7 **Bathe, K. J.** Conserving energy and momentum in nonlinear dynamics: a simple implicit time integration scheme. *Comput. Struct.*, 2007, **85**, 437–445.

8 **Wilson, E. L., Farhoomand, I.,** and **Bathe, K. J.** Nonlinear dynamic analysis of complex structures. *Earthquake Eng. Struct. Dyn.*, 1973, **1**, 241–252.

9 **Hilber, H. M., Hughes, T. J. R.,** and **Taylor, R. L.** Improved numerical dissipation for time integration algorithms in

structural dynamics. *Earthquake Eng. Struct. Dyn.*, 1977, **5**, 283–292.
10 **Wood, W. L., Bossak, M.,** and **Zienkiewicz, O. C.** An alpha modification of Newmark's method. *Int. J. Numer. Meth. Eng.*, 1981, **15**, 1562–1566.
11 **Bazzi, G.** and **Anderheggen, E.** The ρ-family of algorithms for time-step integration with improved numerical dissipation. *Earthquake Eng. Struct. Dyn.*, 1982, **10**, 537–550.
12 **Chung, J.** and **Hulbert, G. M.** A time integration algorithm for structural dynamics with improved numerical dissipation: the generalized-α method. *J. Appl. Mech-T ASME*, 1993, **60**, 371–375.
13 **Fung, T. C.** Weighting parameters for unconditionally stable higher-order accurate time step integration algorithms. Part 1-first-order equations. *Int. J. Numer. Meth. Eng.*, 1999, **45**, 941–970.
14 **Rezaiee-Pajand, M.** and **Alamatian, J.** Implicit higher-order accuracy method for numerical integration in dynamic analysis. *J. Struct. Eng. ASCE*, 2008, **134**(6), 973–985.
15 **Chien, C. C., Yang, C. S.,** and **Tang, J. H.** Three-dimensional transient elastodynamic analysis by a space and time-discontinuous Galerkin finite element method. *Finite Elem. Anal. Des.*, 2003, **39**, 561–580.
16 **Wang, M. F.** and **Au, F. T. K.** Higher-order mixed method for time integration in dynamic structural analysis. *J. Sound Vibr.*, 2004, **278**, 690–698.
17 **Kunthong, P.** and **Thompson, L. L.** An efficient solver for the high-order accurate time-discontinuous Galerkin (TDG) method for second-order hyperbolic systems. *Finite Elem. Anal. Des.*, 2005, **41**, 729–762.
18 **Razavi, S. H., Abolmaali, A.,** and **Ghassemieh, M.** A weighted residual parabolic acceleration time integration method for problems in structural dynamics. *Comput. Meth. Appl. Math.*, 2007, **7**(3), 227–238.
19 **Krenk, S.** State-space time integration with energy control and fourth-order accuracy for linear dynamic systems. *Int. J. Numer. Meth. Eng.*, 2006, **65**, 595–619.
20 **Idesman, A. V., Schmidt, M.,** and **Sierakowski, R. L.** A new explicit predictor–multicorrector high-order accurate method for linear elastodynamics. *J. Sound Vibr.*, 2008, **310**, 217–229.
21 **Soleymani Shishvan, S., Noorzad, A.,** and **Ansari, A.** A time integration algorithm for linear transient analysis based on the reproducing kernel method. *Comput. Meth. Appl. Mech. Eng.*, 2009, **198**(41–44), 3361–3377.
22 **Möller, P. W.** High-order hierarchical A- and L-stable integration methods. *Int. J. Numer. Meth. Eng.*, 1993, **36**, 2607–2624.
23 **Fung, T. C.** Unconditionally stable higher-order accurate Hermitian time finite elements. *Int. J. Numer. Meth. Eng.*, 1996, **39**, 3475–3495.
24 **Fung, T. C.** Third-order time-step integration methods with controllable numerical dissipation. *Commun. Numer. Meth. Eng.*, 1997, **13**, 307–315.
25 **Fung, T. C.** Complex-time-step Newmark methods with controllable numerical dissipation. *Int. J. Numer. Meth. Eng.*, 1998, **41**, 65–93.
26 **Fung, T. C.** Weighting parameters for unconditionally stable higher-order accurate time step integration algorithms, part 2–second-order equations. *Int. J. Numer. Meth. Eng.*, 1999, **45**, 971–1006.
27 **Wang, M. F.** and **Au, F. T. K.** On the precise integration methods based on Padé approximations. *Comput. Struct.*, 2009, **87**, 380–390.
28 **Dahlquist, G. G.** A special stability problem for linear multistep methods. *BIT*, 1963, **3**(1), 27–43.
29 **Austin, M.** High-order integration of smooth dynamical systems: theory and numerical experiments. *Int. J. Numer. Meth. Eng.*, 1993, **36**, 2107–2122.
30 **Tarnow, N.** and **Simo, J. C.** How to render second order accurate time-stepping algorithms fourth order accurate while retaining the stability and conservation properties. *Comput. Meth. Appl. Mech. Eng.*, 1994, **115**, 233–252.
31 **Hoff, C.** and **Taylor, R. L.** Higher derivative explicit one step methods for non-linear dynamic problems. Part I: design and theory. *Int. J. Numer. Meth. Eng.*, 1990, **29**, 275–290.
32 **Cheng, F. Y.** *Matrix analysis of structural dynamics: applications and earthquake engineering*, 2000 (Marcel Dekker, Inc., New York, USA).
33 **Bathe, K. J.** *Finite element procedures*, 1996 (Prentice-Hall Inc., USA).
34 **Rezaiee-Pajand, M.** and **Alamatian, J.** Nonlinear dynamic analysis by dynamic relaxation method. *Struct. Eng. Mech.*, 2008, **28**(5), 549–570.
35 **Qiang, S.** An adaptive dynamic relaxation method for nonlinear problems. *Comput. Struct.*, 1988, **30**(4), 855–859.
36 **Underwood, P.** Dynamic relaxation. In *Computational method for transient analysis* (Eds T. Belytschko and T. J. R. Hughes), 1983, pp. 245–265 (Elsevier, Amsterdam).
37 **Papadrakakis, M.** A method for automatic evaluation of the dynamic relaxation parameters. *Comput. Meth. Appl. Mech. Eng.*, 1981, **25**, 35–48.
38 **Onate, E., Zienkiewicz, O. C., Suarez, B.,** and **Taylor, R. L.** A general methodology for deriving shear constrained Reissner-Mindlin plate elements. *Int. J. Numer. Meth. Eng.*, 1992, **33**, 345–367.

APPENDIX

Notation

c_f	fictitious damping coefficient
$\mathbf{C}, \mathbf{C}_F$	real and fictitious damping matrices
$\mathbf{M}, \mathbf{M}_F$	real and fictitious mass matrices
N_{ij}	coefficients of the Newton interpolation
$\boldsymbol{P}$	force vector
$\boldsymbol{R}$	residual force vector
$\mathbf{S}$	stiffness matrix
t, τ	real and artificial time
T	natural period of system
$\boldsymbol{X}, \dot{\boldsymbol{X}}, \ddot{\boldsymbol{X}}$	displacement, velocity, and acceleration vectors
$\Delta t, \Delta\tau$	real and artificial time step value
λ_i	eigenvalue
ρ	spectral radius
ω	natural angular frequency